

Monte Carlo Simulations in Multibaric-Multithermal Ensemble

Hisashi Okumura^{1;} and Yuko Okamoto^{1;2;y}

¹Department of Theoretical Studies
Institute for Molecular Science
Okazaki, Aichi 444-8585, Japan

²Department of Functional Molecular Science
The Graduate University for Advanced Studies
Okazaki, Aichi 444-8585, Japan

We propose a new generalized-ensemble algorithm, which we refer to as the multibaric-multithermal Monte Carlo method. The multibaric-multithermal Monte Carlo simulations perform random walks widely both in volume space and in potential energy space. From only one simulation run, one can calculate isobaric-isothermal-ensemble averages at any pressure and any temperature. We test the effectiveness of this algorithm by applying it to the Lennard-Jones 12-6 potential system with 500 particles. It is found that a single simulation of the new method indeed gives accurate average quantities in isobaric-isothermal ensemble for a wide range of pressure and temperature.

PACS numbers: 64.70.Fx, 02.70.Ns, 47.55.Dz

Monte Carlo (MC) algorithm is one of the most widely used methods of computational physics. In order to realize desired statistical ensembles, corresponding MC techniques have been proposed [1, 2, 3, 4, 5]. The first MC simulation was performed in the canonical ensemble in 1953 [1]. This method is called the Metropolis algorithm and widely used. The canonical probability distribution $P_{NVT}(E)$ for potential energy E is given by the product of the density of states $n(E)$ and the Boltzmann weight factor $e^{-\beta E}$:

$$P_{NVT}(E) = n(E) e^{-\beta E}; \quad (1)$$

where β is the inverse of the product of the Boltzmann constant k_B and temperature T_0 at which simulations are performed. Since $n(E)$ is a rapidly increasing function and the Boltzmann factor decreases exponentially, $P_{NVT}(E)$ is a bell-shaped distribution.

The isobaric-isothermal MC simulation [2] is also extensively used. This is because most experiments are carried out under the constant pressure and constant temperature conditions. Both potential energy E and volume V fluctuate in this ensemble. The distribution $P_{NPT}(E; V)$ for E and V is given by

$$P_{NPT}(E; V) = n(E; V) e^{-\beta H}; \quad (2)$$

Here, the density of states $n(E; V)$ is given as a function of both E and V , and H is the "enthalpy":

$$H = E + P_0 V; \quad (3)$$

where P_0 is the pressure at which simulations are performed. This ensemble has bell-shaped distributions in both E and V .

Besides the above physical ensembles, it is now almost a default to simulate in artificial, generalized ensembles so that the multiple-minima problem, or the broken ergodicity problem, in complex systems can be overcome (for a recent review, see Ref. [6]). The multicanonical algorithm [7, 8] is one of the most well known such methods in generalized ensemble. In multicanonical ensemble, a non-Boltzmann weight factor $W_{mc}(E)$ is used. This multicanonical weight factor is characterized by a flat probability distribution $P_{mc}(E)$:

$$P_{mc}(E) = n(E) W_{mc}(E) = \text{constant}; \quad (4)$$

and thus a free random walk is realized in the potential energy space. This enables the simulation to escape from any local-minimum-energy state and to sample the configurational space more widely than the conventional canonical MC algorithm. Another advantage is that one can obtain various canonical ensemble averages at any temperature from a

^E Electronic address: hokumura@im.s.ac.jp

^y Electronic address: okamotoy@im.s.ac.jp

single simulation run by the reweighting techniques [9]. This method is now widely used in complex systems such as proteins and glasses [6]. However, it is difficult to compare the simulation conditions with experimental environments of constant pressure, since the simulations are performed in a fixed volume.

In this Letter, we propose a new MC algorithm in which one can obtain various isobaric-isothermal ensembles from only one simulation. In other words, we introduce the idea of the multicanonical technique into the isobaric-isothermal ensemble MC method. We call this method the multibaric-multithermal algorithm. This MC simulation performs random walks in volume space as well as in potential energy space. As a result, this method has the following advantages: (1) It allows the simulation to escape from any local minimum-energy state and to sample the configurational space more widely than the conventional isobaric-isothermal method. (2) One can obtain various isobaric-isothermal ensembles not only at any temperature, as in the multicanonical algorithm, but also at any pressure from only one simulation run. (3) One can control pressures and temperatures similarly to real experimental conditions.

In the multibaric-multithermal ensemble, every state is sampled by a weight factor $W_{mbt}(E;V) \exp[-\beta H_{mbt}(E;V)g]$ (H_{mbt} is referred to as the multibaric-multithermal enthalpy) so that a uniform distribution in both potential energy space and volume space is obtained:

$$P_{mbt}(E;V) = n(E;V)W_{mbt}(E;V) = \text{constant} : \quad (5)$$

We call $W_{mbt}(E;V)$ the multibaric-multithermal weight factor.

In order to perform the multibaric-multithermal MC simulation, we follow the conventional isobaric-isothermal MC techniques [2]. In this method, we perform Metropolis sampling on the scaled coordinates $s_i = L^{-1}r_i$ (r_i are the real coordinates) and the volume V (here, the particles are placed in a cubic box of a side of size $L = \sqrt[3]{V}$). The trial moves of the scaled coordinates from s_i to s_i^0 and of the volume from V to V^0 are generated by uniform random numbers. The enthalpy is accordingly changed from $H(E(s^{(N)};V);V)$ to $H^0(E(s^{(0N)};V^0);V^0)$ by these trial moves. The trial moves will be accepted with the probability

$$\text{acc}(o \rightarrow n) = \min(1; \exp[-\beta(H^0 - H - N k_B T_0 \ln(V^0/V)g)]) ; \quad (6)$$

where N is the total number of particles in the system.

Replacing H by H_{mbt} , we can perform the multibaric-multithermal MC simulation. The trial moves of s_i and V are generated in the same way as in the isobaric-isothermal MC simulation. The multibaric-multithermal enthalpy is changed from $H_{mbt}(E(s^{(N)};V);V)$ to $H_{mbt}^0(E(s^{(0N)};V^0);V^0)$ by these trial moves. The trial moves will now be accepted with the probability

$$\text{acc}(o \rightarrow n) = \min(1; \exp[-\beta(H_{mbt}^0 - H_{mbt} - N k_B T_0 \ln(V^0/V)g)]) : \quad (7)$$

The multibaric-multithermal probability distribution $P_{mbt}(E;V)$ is obtained by this scheme.

In order to calculate the isobaric-isothermal ensemble average, we employ the reweighting techniques [9]. The probability distribution $P_{NPT}(E;V;T;P)$ at any temperature T and any pressure P in the isobaric-isothermal ensemble is given by

$$P_{NPT}(E;V;T;P) = \frac{\int dV \int dE P_{mbt}(E;V) W_{mbt}^{-1}(E;V) e^{-\beta(E+PV)}}{\int dV \int dE P_{mbt}(E;V) W_{mbt}^{-1}(E;V) e^{-\beta(E+PV)}} : \quad (8)$$

The expectation value of a physical quantity A at T and P is estimated from

$$\begin{aligned} \langle A \rangle_{NPT} &= \frac{\int dV \int dE A(E;V) P_{NPT}(E;V;T;P)}{\int dV \int dE P_{NPT}(E;V;T;P)} ; \\ &= \frac{\langle A(E;V) W_{mbt}^{-1}(E;V) e^{-\beta(E+PV)} \rangle_{mbt}}{\langle W_{mbt}^{-1}(E;V) e^{-\beta(E+PV)} \rangle_{mbt}} ; \end{aligned} \quad (9)$$

where $\langle \rangle_{mbt}$ is the multibaric-multithermal ensemble average.

After having given the formalism of the multibaric-multithermal algorithm, let us now describe the process for determining the weight factor $W_{mbt}(E;V)$. This is obtained by the usual iteration of short simulations [10, 11, 12]. The first simulation is carried out at T_0 and P_0 in the isobaric-isothermal ensemble. Namely, we use

$$W_{mbt}^{(1)}(E;V) = \exp[-\beta H_{mbt}^{(1)}(E;V)g] ; \quad (10)$$

where

$$H_{m\text{bt}}^{(1)}(E;V) = E + P_0 V; \quad (11)$$

The i -th simulation is performed with the weight factor $W_{m\text{bt}}^{(i)}(E;V)$ and let $P_{m\text{bt}}^{(i)}(E;V)$ be the obtained distribution. The $(i+1)$ -th weight factor $W_{m\text{bt}}^{(i+1)}(E;V)$ is then given by

$$W_{m\text{bt}}^{(i+1)}(E;V) = \exp f_{0H_{m\text{bt}}^{(i+1)}(E;V)g}; \quad (12)$$

where

$$H_{m\text{bt}}^{(i+1)}(E;V) = \begin{cases} < 8 \\ < H_{m\text{bt}}^{(i)}(E;V) + k_B T_0 \ln P_{m\text{bt}}^{(i)}(E;V); \text{ for } P_{m\text{bt}}^{(i)}(E;V) > 0; \\ : H_{m\text{bt}}^{(i)}(E;V); & \text{ for } P_{m\text{bt}}^{(i)}(E;V) = 0; \end{cases} \quad (13)$$

For convenience, we make E and V discrete into bins and use histograms to calculate $P_{m\text{bt}}^{(i)}(E;V)$. We iterate this process until a reasonably flat distribution $P_{m\text{bt}}^{(i)}(E;V)$ is obtained. After an optimal weight factor is determined, a long simulation is performed to sample the configurational space.

We now present the results of our multibaric-multithermal simulation. We considered a Lennard-Jones 12-6 potential system. We used 500 particles ($N = 500$) in a cubic unit cell with periodic boundary conditions. The length and the energy are scaled in units of the Lennard-Jones diameter and the minimum value of the potential, respectively. We use an asterisk (*) for the reduced quantities such as the reduced length $r = r^*$, the reduced temperature $T = k_B T^*$, the reduced pressure $P = P^*$, and the reduced number density $\rho = \rho^*$ ($N = V$).

We started the multibaric-multithermal weight factor determination of Eqs. (12) and (13) from a regular isobaric-isothermal simulation at $T_0 = 2.0$ and $P_0 = 3.0$. These temperature and pressure are respectively higher than the critical temperature T_c and the critical pressure P_c [13, 14, 15, 16, 17, 18]. Recent reliable data are $T_c = 1.3207(4)$ and $P_c = 0.1288(5)$ [18]. The cutoff radius r_c was taken to be $L/2$. A cutoff correction was added for the pressure and potential energy. In one MC sweep we made the trial moves of all particle coordinates and the volume ($N+1$ trial moves altogether). For each trial move the Metropolis evaluation of Eq. (7) was made. In order to obtain a flat probability distribution $P_{m\text{bt}}(E;V)$, we carried out the MC simulations of 100,000 MC sweeps and iterated the process of Eqs. (12) and (13). In the present case, it was required to make 12 iterations to get an optimal weight factor $W_{m\text{bt}}(E;V)$. We then performed a long multibaric-multithermal MC simulation of 400,000 MC sweeps with this $W_{m\text{bt}}(E;V)$.

For the purpose of comparisons of the new method with the conventional one, we also performed the conventional isobaric-isothermal MC simulations of 100,000 MC sweeps with 500 Lennard-Jones 12-6 potential particles at several sets of temperature and pressure. The temperature ranged from $T = 1.6$ to 2.6 and the pressure from $P = 2.2$ to 3.8.

In order to estimate the statistical accuracies, we performed these MC simulations from four different initial conditions in both multibaric-multithermal and isobaric-isothermal simulations. The error bars were calculated by the standard deviations from these different simulations.

Figure 1 shows the probability distributions of E/N and V/N . Figure 1(a) is the probability distribution $P_{NPT}(E/N;V/N)$ from the isobaric-isothermal simulation first carried out in the process of Eqs. (10) and (11) (i.e., $T_0 = 2.0$ and $P_0 = 3.0$). It is a bell-shaped distribution. On the other hand, Fig. 1(b) is the probability distribution $P_{m\text{bt}}(E/N;V/N)$ from the multibaric-multithermal simulation finally performed. It shows a flat distribution, and the multibaric-multithermal MC simulation indeed sampled the configurational space in wider ranges of energy and volume than the conventional isobaric-isothermal MC simulation.

Figure 2 shows the time series of E/N . Figure 2(a) gives the results of the conventional isobaric-isothermal simulations at $(T;P) = (1.6;3.0)$ and $(2.4,3.0)$, while Figure 2(b) presents those of the multibaric-multithermal simulation. The potential energy fluctuates in narrow ranges in the conventional isobaric-isothermal MC simulations. They fluctuate only in the ranges of $E/N = 4.0 \sim 3.6$ and $E/N = 5.1 \sim 4.7$ at the higher temperature of $T = 2.4$ and at the lower temperature of $T = 1.6$, respectively. On the other hand, the multibaric-multithermal MC simulation performs a random walk that covers a wide energy range.

A similar situation is observed in the time series of V/N . In Fig. 3(a) we show the results of the conventional isobaric-isothermal simulations at $(T;P) = (2.0;2.2)$ and $(2.0,3.8)$, while in Figure 3(b) we give those of the multibaric-multithermal simulation.

The volume fluctuations in the conventional isobaric-isothermal MC simulations are only in the range of $V/N = 1.3 \sim 1.4$ and $V/N = 1.5 \sim 1.6$ at $P = 3.8$ and at $P = 2.2$, respectively. On the other hand, the multibaric-multithermal MC simulation performs a random walk that covers even a wider volume range.

We calculated the ensemble averages of potential energy per particle, $\langle E \rangle_{NPT}$, and density, $\langle \rho \rangle_{NPT}$, at various temperature and pressure values by the reweighting techniques of Eq. (9). They are shown in Fig. 4 and in Fig. 5, respectively. The error bars are smaller than the plots for both cases. The agreement between the multibaric-multithermal data and isobaric-isothermal data are excellent in both $\langle E \rangle_{NPT}$ and $\langle \rho \rangle_{NPT}$.

The important point is that we can obtain any desired isobaric-isothermal distribution in wide temperature and pressure ranges ($T = 1.6 - 2.6$, $P = 2.2 - 3.8$) from a single simulation run by the multibaric-multithermal MC algorithm. This is an outstanding advantage over the conventional isobaric-isothermal MC algorithm, in which simulations have to be carried out separately at each temperature and pressure, because the reweighting techniques based on the isobaric-isothermal simulations can give correct results only for narrow ranges of temperature and pressure values.

Figures 4 and 5 also show two equations of states of the Lennard-Jones 12-6 potential fluid. One is determined by Johnson et al. [19] and the other by Sun and Teja [20]. These equations are determined by fitting procedure to the molecular simulation results. Our multibaric-multithermal simulation results agree very well with those of these equations. Investigating in more detail, however, the two equations give slightly different results. Most of our data lie in between them.

In conclusion, we proposed a new MC algorithm that is based on multibaric-multithermal ensemble. We applied this method to the Lennard-Jones 12-6 potential system. The advantage of this method is that the simulation performs random walks in both potential energy space and volume space and sample the configurational space much more widely than the conventional isobaric-isothermal MC method. Therefore, one can obtain various isobaric-isothermal ensemble averages at any desired temperature and pressure from only one simulation run. This allows one to specify a pressure and to compare simulation conditions directly with those of real experiments. The multibaric-multithermal algorithm will thus be of great use for investigating a large variety of complex systems such as proteins, polymers, supercooled liquids, and glasses. It will be particularly useful for the study of, for example, pressure induced phase transitions.

We would like to thank M. M. Kamio of National Institute of Advanced Industrial Science and Technology and U. H. E. Hansmann of Michigan Technological University for useful discussions at the early stage of the present work.

-
- [1] N. Metropolis, A. W. Rosenbluth, M. N. Rosenbluth, A. H. Teller, and E. Teller, *J. Chem. Phys.* 21, 1087 (1953).
 - [2] I. R. McDonald, *Mol. Phys.* 23, 41 (1972).
 - [3] M. Creutz, *Phys. Rev. Lett.* 50, 1411 (1983).
 - [4] M. P. Allen and D. J. Tildesley, *Computer Simulation of Liquids*, (Clarendon Press, Oxford, 1987) p. 110.
 - [5] D. Frenkel and B. Smith, *Understanding Molecular Simulation From Algorithms to Applications*, (Academic Press, San Diego, 2002) p. 111.
 - [6] A. Mitsutake, Y. Sugita, and Y. Okamoto, *Biopolymers (Peptide Science)* 60, 96 (2001).
 - [7] B. A. Berg and T. Neuhaus, *Phys. Lett. B* 267, 249 (1991).
 - [8] B. A. Berg and T. Neuhaus, *Phys. Rev. Lett.* 68, 9 (1992).
 - [9] A. M. Ferrenberg and R. H. Swendsen, *Phys. Rev. Lett.* 61, 2635 (1988); *ibid.* 63, 1658 (E) (1989).
 - [10] B. A. Berg and T. Celik, *Phys. Rev. Lett.* 69, 2292 (1992).
 - [11] J. Lee, *Phys. Rev. Lett.* 71, 211 (1993); *ibid.* 2353 (E) (1993).
 - [12] Y. Okamoto and U. H. E. Hansmann, *J. Phys. Chem.* 99, 11276 (1995).
 - [13] H. Okumura and F. Yonezawa, *J. Chem. Phys.* 113, 9162 (2000).
 - [14] H. Okumura and F. Yonezawa, *J. Phys. Soc. Jpn.* 70, 1006 (2001).
 - [15] A. Z. Panagiotopoulos, *J. Phys.: Condens. Matter* 12, R25 (2000).
 - [16] J. M. Caillol, *J. Chem. Phys.* 109, 4885 (1998).
 - [17] J. J. Poto and A. Z. Panagiotopoulos, *J. Chem. Phys.* 109, 10914 (1998).
 - [18] H. Okumura and F. Yonezawa, *J. Phys. Soc. Jpn.* 70, 1990 (2001).
 - [19] J. K. Johnson, J. A. Zollweg, and K. E. Gubbins, *Mol. Phys.* 78, 591 (1993).
 - [20] T. Sun and A. S. Teja, *J. Phys. Chem.* 100, 17365 (1996).

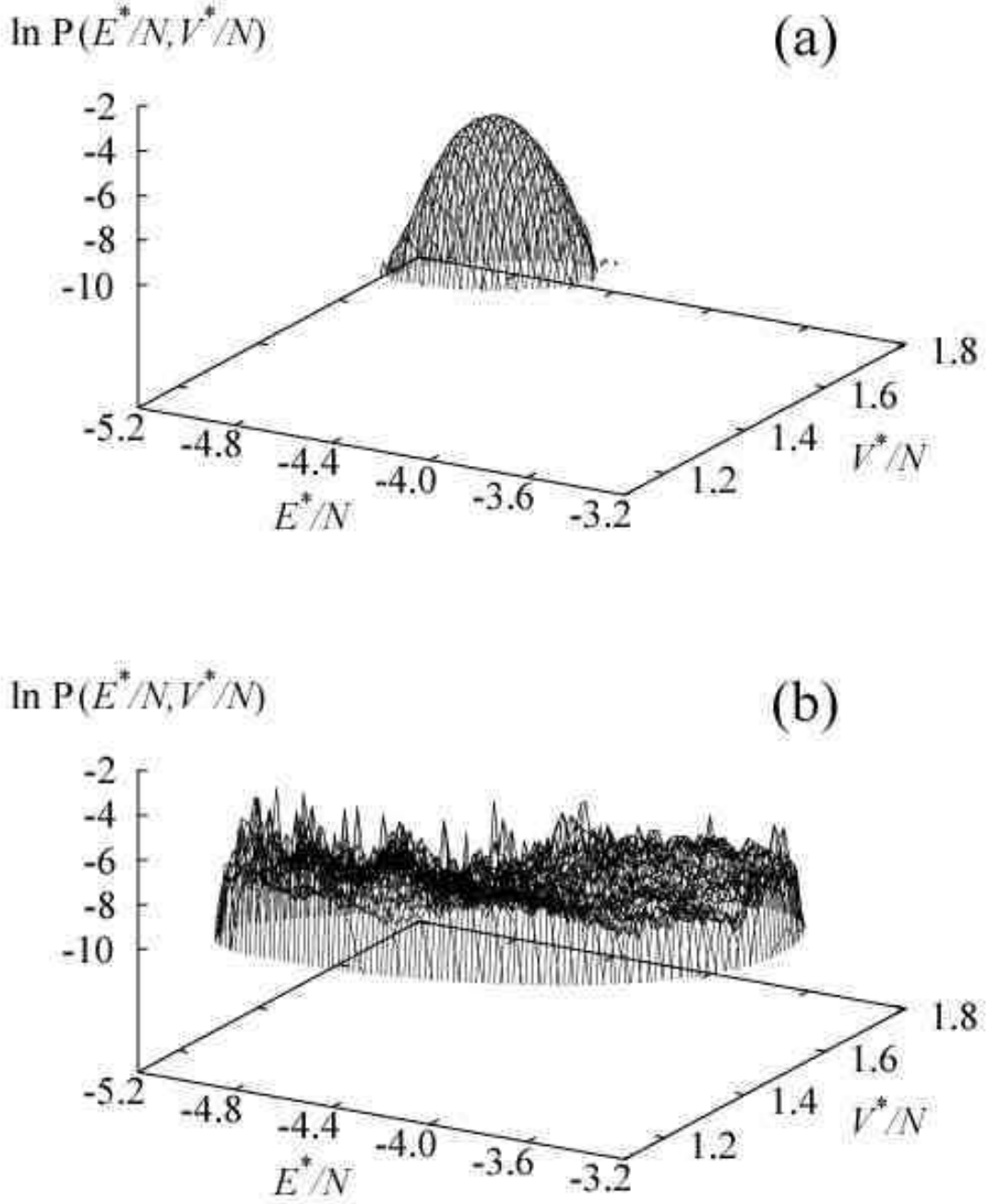


FIG. 1: (a) The probability distribution $P_{NPT}(E^*/N; V^*/N)$ in the isobaric-isothermal simulation at $(T^*; P^*) = (T_0; P_0) = (2.0; 3.0)$ and (b) the probability distribution $P_{mbt}(E^*/N; V^*/N)$ in the multibarc-multithermal simulation.

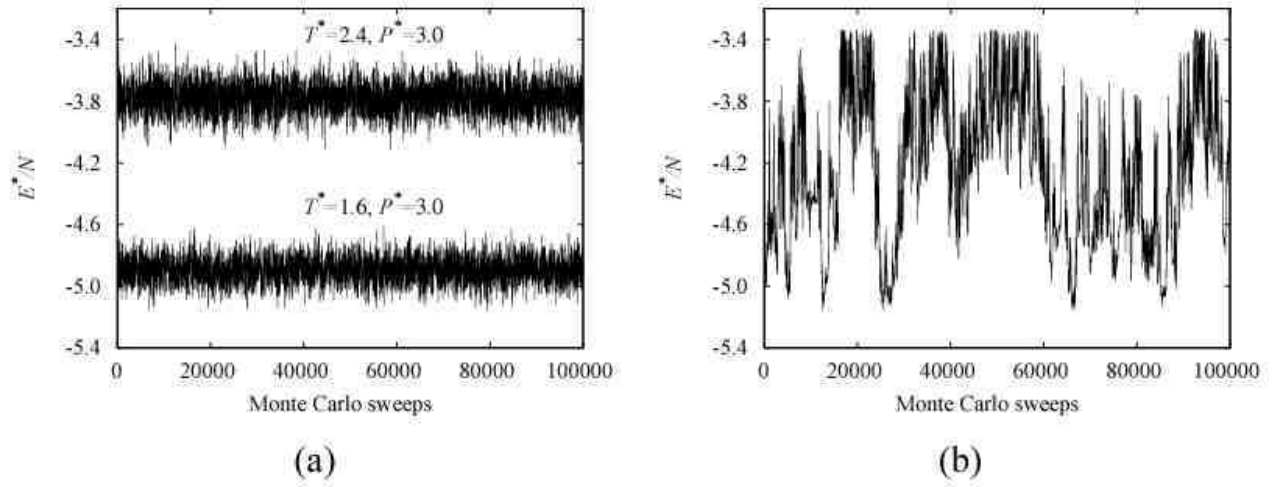


FIG. 2: The time series of E^*/N from (a) the conventional isobaric-isotherm alMC simulations at $(T^*; P^*) = (2.4; 3.0)$ and at $(T^*; P^*) = (1.6; 3.0)$ and (b) the multibarc-multitherm alMC simulation.

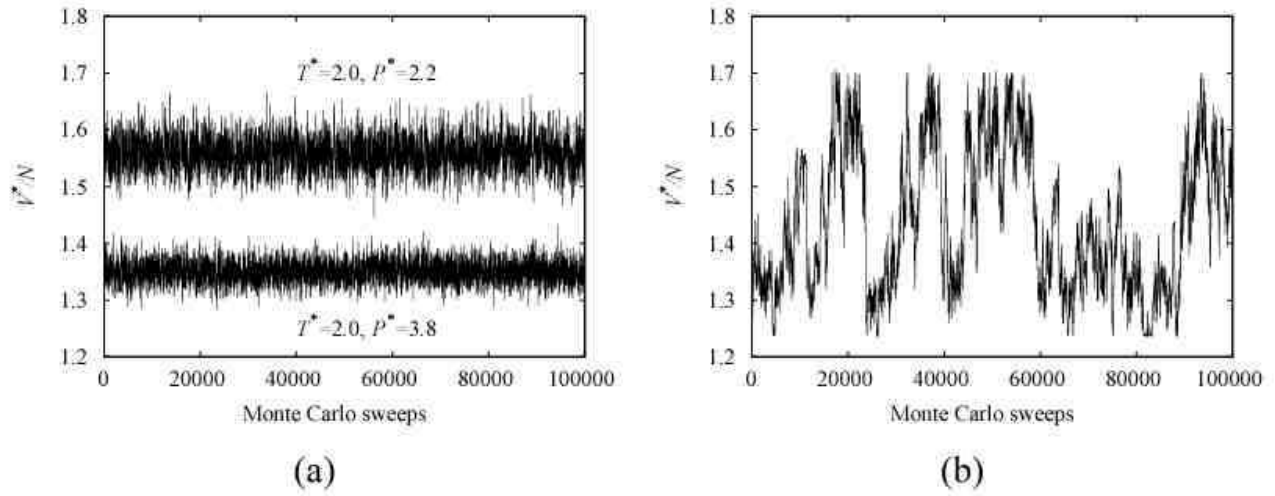


FIG. 3: The time series of V^*/N from (a) the conventional isobaric-isotherm alMC simulations at $(T^*; P^*) = (2.0; 2.2)$ and at $(T^*; P^*) = (2.0; 3.8)$ and (b) the multibarc-multitherm alMC simulation.

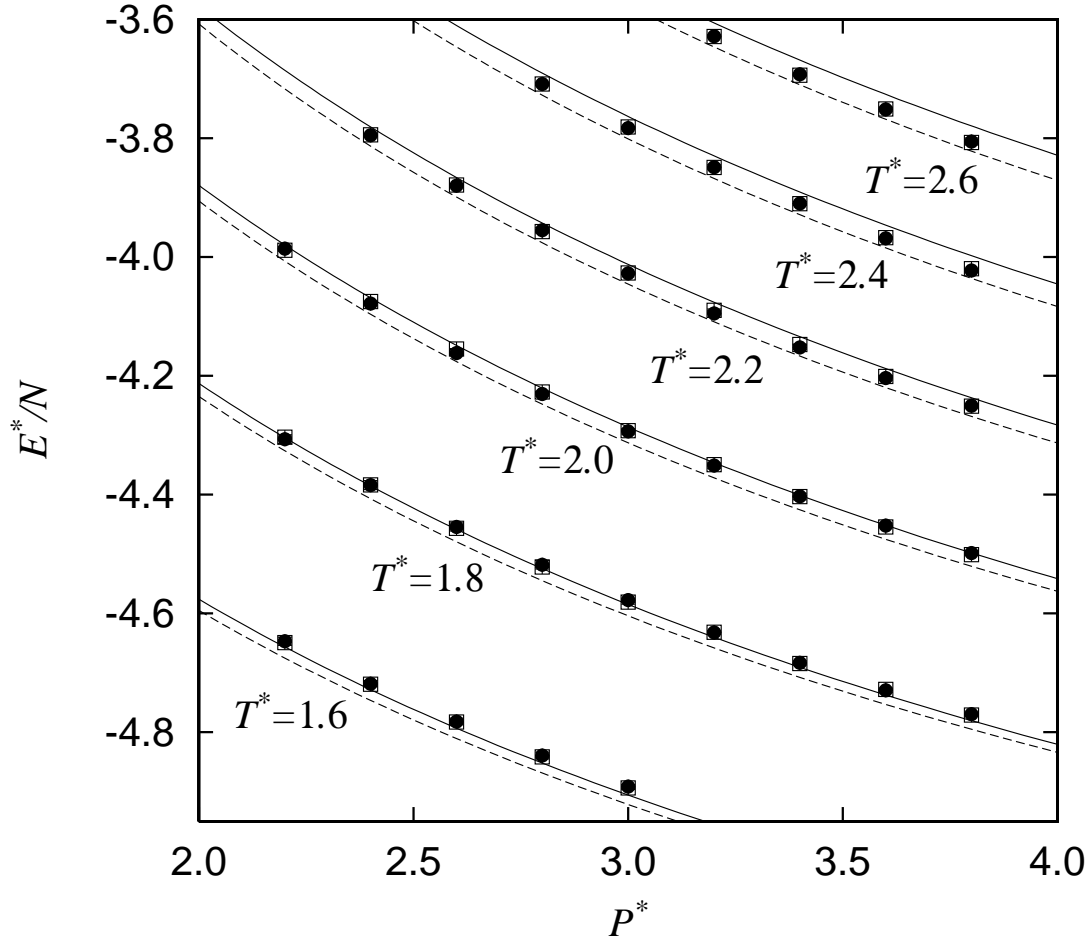


FIG. 4: Average potential energy per particle $\langle E^*/N \rangle_{NPT}$ at various temperature and pressure values. Filled circles: Multibaric-multitherm alMC simulations. Open squares: Conventional isobaric-isotherm alMC simulations. Solid line: Equation of states calculated by Johnson et al. [19]. Broken line: Equation of states calculated by Sun and Teja [20].

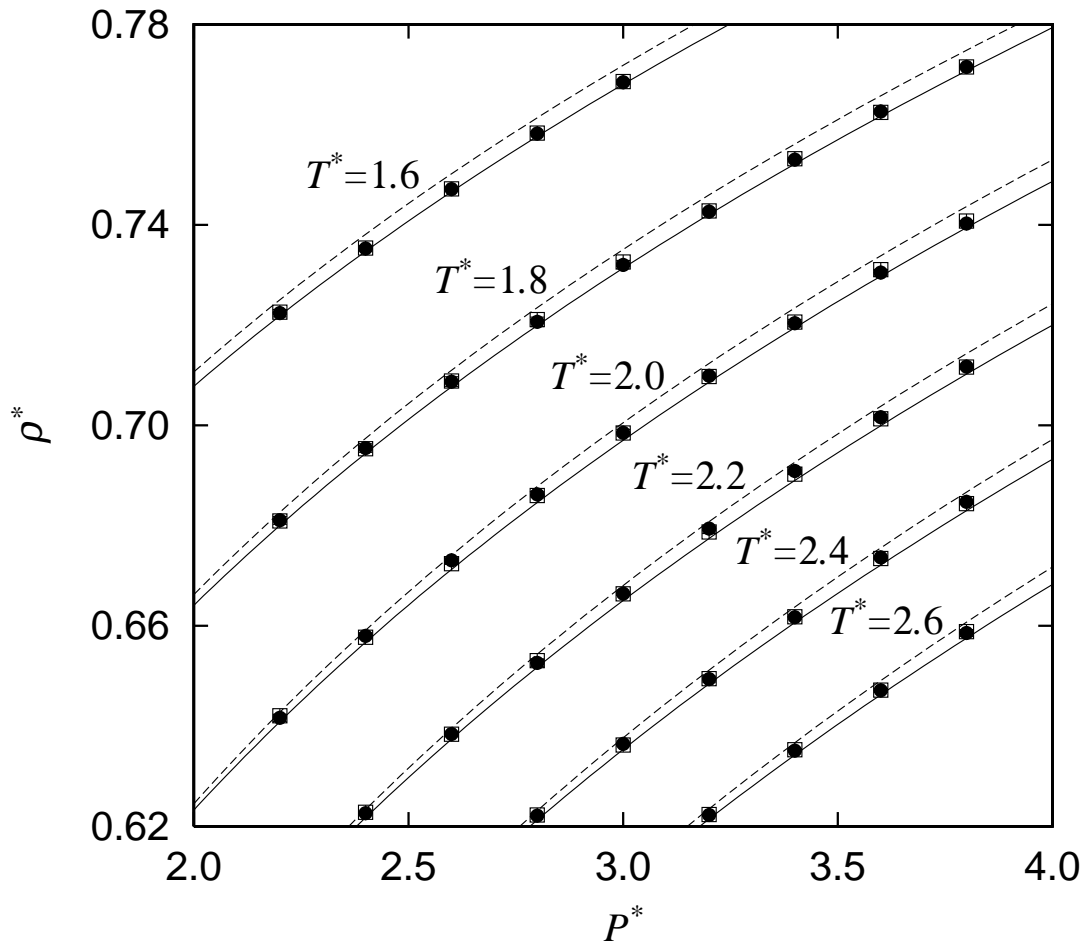


FIG . 5: Average density $\langle \rho \rangle_{NPT}$ at various temperature and pressure values. See the caption of Fig. 4 for details.